New Type of Nitrides with High Electrical and Thermal Conductivities

CHIN. PHYS. LETT. Vol. 35, No. 8 (2018) 087102

New Type of Nitrides with High Electrical and Thermal Conductivities *

Ning Liu(刘宁)[1,2], Xiaolong Chen(陈小龙)[1,2,3**], Jiangang Guo(郭建刚)[1**],
Jun Deng(邓俊)[1,2], Liwei Guo(郭丽伟)[1]

[1] *Research & Development Center for Functional Crystals, Laboratory of Advanced Materials & Electron Microscopy, Beijing National Laboratory for Condensed Matter Physics, Institute of Physics, Chinese Academy of Sciences, Beijing 100190*
[2] *University of Chinese Academy of Sciences, Beijing 100049*
[3] *Collaborative Innovation Center of Quantum Matter, Beijing 100084*

(Received 28 May 2018)

The nitrogen dimer as both a fundamental building unit in designing a new type of nitrides, and a material gene associated with high electrical and thermal conductivities is investigated by first principles calculations. The results indicate that the predicted SiN_4 is structurally stable and reasonably energy-favored with a striking feature in its band structure that exhibits free electron-like energy dispersions. It possesses a high electrical conductivity (5.07×10^5 S/cm) and a high thermal conductivity (371 W/m·K) comparable to copper. The validity is tested by isostructural AlN_4 and SiC_4. It is demonstrated that the nitrogen dimers can supply a high density of delocalized electrons in this new type of nitrides.

PACS: 71.20.Ps, 72.15.Eb, 78.40.Kc DOI: 10.1088/0256-307X/35/8/087102

Considerable progress in material prediction has been achieved over the last decade owing to the development of the high throughput calculations and machine learning algorithms.[1,2] Genes of materials or fingerprints that encode the information of crystallography, chemistry of constitutional elements, electronic band structure etc., were identified by analyzing known material spaces and were used to successfully predict new compounds with desired properties in several specific classes of functional materials.[3–7] Although recent breakthroughs in artificial intelligence allow self-learning without human knowledge in mastering games,[8,9] the machine learning in the field of material prediction is highly dependent on the training samples, and experts' knowledge is a prerequisite.[1] A concern arises, of whether the training samples are diverse and representative enough to construct effective and efficient learning algorithms. It will be of importance to add training samples to cover previously unknown samples.

In the present work we explore a new type of nitrides with high electrical and thermal conductivities while they are lattice dynamically stable and energy favored. Our focus is on the compounds that contain delocalized electrons from the non-metal elements. These delocalized electrons are known to play a vital role in determining the conductivity of graphite,[10] graphene,[11] and conductive polymers.[12] These delocalized electrons come from π bonds forming by p subshell electrons. It is the π bonds that lead to the emergent Dirac cones with a zero gap in graphene[13] and relatively narrow-band gaps in conductive polymers. However, they are usually semiconductors and made conductive only by heavy doping of either electrons or holes.[14] So do degenerate semiconductors.[15] Semimetals are another class of conductive solids due to a small overlap between their conduction band bottoms and their valence band tops in terms of energy. Compared to metals or alloys, graphene, conductive polymers, and semimetals are still poor electrical conductors as they do not have a high density of delocalized electrons. Further enhancing conductivity is often limited by the solid solubility and structural stability. To the best of our knowledge, no compounds consisting of non-metal elements have been known to be intrinsic conductors.[16]

In this Letter, we investigate the material gene in a compound consisting of only non-metal elements to realize intrinsic metallic characteristics using first-principles calculations. We show that SiN_4, a binary compound with diamond-like structure consisting of two of the most abundant elements on the earth, has high electrical and thermal conductivities comparable to metals such as Cu and Al without doping. This cubic compound is stable in the lattice dynamic and reasonably favored in cohesive energy. Its electronic band structure resembles that of a monovalent metal due to the existence of delocalized electrons. AlN_4, an isostructural compound, possesses similar properties with SiN_4. Our results demonstrate that nitrogen dimer, formed with double bonds, can be used as a material gene to construct a new class of materials with high electric and thermal conductivities.

In designing such a compound, our consideration

*Supported by the National Natural Science Foundation of China under Grant Nos 51532010, 91422303, 51672306 and 51772322, the National Key Research and Development Program of China under Grant No 2016YFA0300604, the Beijing Municipal Science & Technology Commission under Grant No Z161100002116018, and the Strategic Priority Research Program of the Chinese Academy of Sciences under Grant No XDB07020100.

**Corresponding author. Email: chenx29@iphy.ac.cn; jgguo@iphy.ac.cn

begins with a material gene that can supply a high density of delocalized electrons. Double N=N bonds, which do exist in some nitrides,[17–19] is a proper choice. Since each N atom has five valence electrons, three electrons will be left over after forming two σ bonds, one involving two neighboring N atoms, the other involving a nitrogen atom and a second element atom to be connected, see the following. Among the three unbounded $2p$ electrons, two of them from p_y and p_z subshells will separately form two π bonds with the neighboring N atom. In this way, the last electron can only stay at the anti-bonding π^* bond since σ and π bonds are fully occupied, finally leading to a double N=N bond.

Next, we consider a proper element needed to be bonded with N atoms. Silicon first comes into our choice due to the fact that α-Si_3N_4[20] and β-Si_3N_4[21] are well known refractory ceramics. In these compounds, Si is bounded by four N atoms, forming a tetrahedron SiN_4 with Si being at the center. Since Si is a semiconductor with a bandgap around 1 eV, its conduction band is not far away from the Fermi level and possibly lies at an energy level close to the π^* band of the double N=N bond. This will be conducive to enhance electrical conductivity. Here the double N=N bond will act as a linker that connects the two SiN_4 tetrahedra.

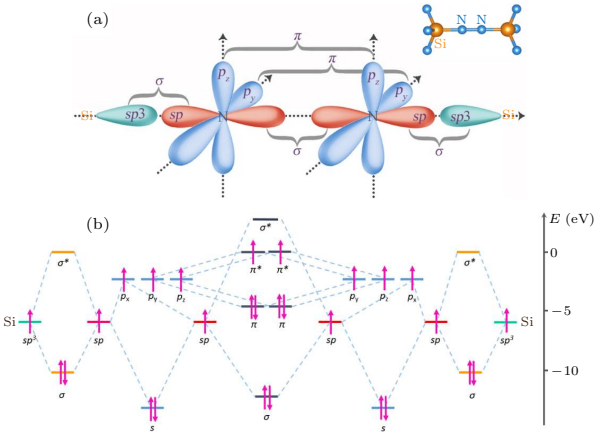

Fig. 1. (a) Schematic orbitals for the formation of a double N=N bond when two SiN_4 tetrahedra are approaching and they are close enough. (b) Electron filling in proposed molecular orbitals including bonding orbitals and anti-bonding orbitals. The double N=N bond comprises one σ bond contributed from the hybridization of sp, two π bonds from p_y and p_z orbitals, and two π^* anti-bonds. Yellow and black bars denote the molecular orbitals of Si-N bonds and N=N bonds, respectively.

Figures 1(a) and 1(b) show schematically how electrons of two nitrogen atoms hybridize and the way they bond. Si is bonded by four N atoms all forming σ bonds from Si sp^3 and N sp hybridizations. According to the octet rule, two σ and two π bonds will comprise the valence bands. The present material is in the half occupation of π^* bonds by delocalized electrons, which is expected to comprise the conduction bands. The anti-bonding σ^* is totally unoccupied in the ground state. The following calculations verify these assumptions.

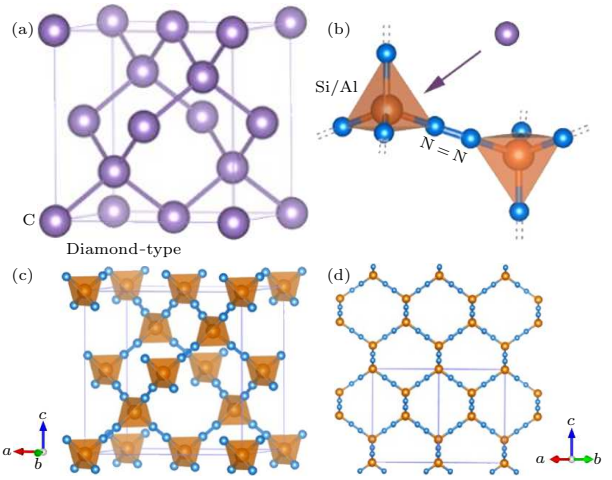

Fig. 2. (a) The crystal structure of diamond with space group $Fd\bar{3}m$ (No. 227). (b) Tetrahedron SiN_4 with each Si/Al atom coordinated by four N atoms. (c) The crystal structure of the SiN_4 compound, which can be regarded as replacing C atoms of diamond with tetrahedron SiN_4 and then each tetrahedron SiN_4 is connected through double N=N bonds by four other SiN_4 tetrahedra. (d) Crystal structure viewed from [110] directions of SiN_4.

With the above considerations in mind, we need to construct a structure that contains both SiN_4 tetrahedron and N=N double bonds. Every SiN_4 tetrahedron should have an identical crystallographic environment and the arrangement of them must meet the translation symmetry. Each SiN_4 bonded by the other four via N=N bonds is the most feasible way in bonding topology. Among all porotypes with every motif connecting each other in this way, the cubic diamond structure possesses the highest symmetry. We then built the structure by replacing carbon atoms in the diamond unit cell with SiN_4 tetrahedra, where Si atoms occupy the positions of C atoms, as shown in Fig. 2, in the same way first put forward by Su *et al.*[22] in constructing the T-carbon. It is noted that the T-carbon was experimentally observed recently.[23] Other analogous 3D carbon allotrope with sp and sp^3 hybridization was also theoretically proposed.[24]

Our calculations were performed using density functional theory[25,26] with ultrasoft pseudopotentials. Both generalized gradient approximation (GGA)[27] and the local density approximation (LDA)[28] were used for the sake of the reliability of calculated results. Other details were deposited in the Supplemental Material. Geometry optimization implemented with the Broyden, Fletcher, Goldfarb, and Shannon (BFGS)[29] method was performed on the structure shown in Fig. 2(c) until the remnant Hellman–Feynman forces on the atoms were less than 0.01 eV/Å. The Si and N atoms are set to occupy the Wyckoff 8(a) site (0, 0, 0) and the Wyckoff 32(c) site (x, x, x) with space group $Fd\bar{3}m$ (No. 227). This gives lattice constant $a = 10.392$ Å and $x = 0.091$. Each

unit contains 8 SiN_4 tetrahedra and the compound has a density of 0.996 g/cm^3. The bond length d_{Si-N} is 1.635 Å, slightly shorter than 1.738 Å observed in α-Si_3N_4.[20] The bond length for d_{N-N} is 1.231 Å, in good agreement with ones found in other nitrides, which contain double N=N bonds.[17–19] SiN_4 is similar in structure to T-carbon[22] and supertetrahedral Al and B recently reported by Getmanskii *et al.*[30,31] However, it does have distinct features from these in fundamental building units (FBU) and bonding topology. Here the FBUs are SiN_4 tetrahedra and N=N dimers. In SiN_4 tetrahedra, Si is located at the center and is coordinated by four N atoms which are not bonded to each other. In both T-carbon and supertetrahedral Al/B, their tetrahedra consists of four C(Al/B) atoms that are all bonded with each other but empty at the center, and are connected by C(Al/B)-C(Al/B) bonds.

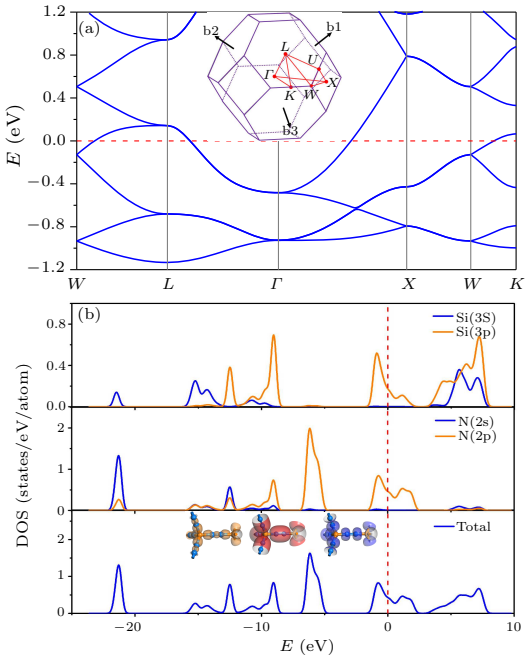

Fig. 3. (a) The electronic band structure of SiN_4, and the inset shows the first Brillouin zone. (b) Partial density of states for atoms Si and N and the total density of states. Inset of the bottom panel shows the molecular orbitals at different energy levels. The π^* anti-bonding orbitals dominate in the vicinity of the Fermi energy, and the π bonding orbitals of N=N appear at -6 eV and the σ bonding orbitals from N=N and N-Si spread over and overlap below -8 eV.

Then we investigate the structural stability in terms of cohesive energy (E_c) and lattice dynamics. The value of E_c is defined as the energy difference between atoms in the corresponding compounds and in a free state. The lower E_c, the stabler a structure. Here E_c for SiN_4 is -7.16 eV/atom (see Table S1 in the Supplementary Material[32]), higher than -8.26 eV/atom for both α and β-Si_3N_4, and -8.11 eV/atom in γ-Si_3N_4[33] obtained under high pressures. However, E_c of N_2 molecular and silicon are -7.92 eV/atom and -5.43 eV/atom, respectively. The relatively high E_c for SiN_4 is due to the existence of double N=N bonds, which is estimated to be about 5.13 eV/bond. However, this cohesive energy would make the structure survive well above room temperature. Our molecular dynamic calculations show that it is stable even at 600 K. The calculated phonon spectra is shown in Fig. S1 in the Supplementary Material.[32] No negative frequency in the lowest acoustical branch is presented either using GGA or LDA, suggesting the stability of the structure. The isostructural BN_4 is not stable in lattice dynamics as evidenced by its negative frequency, implying the stability of tetrahedron contributes significantly to the formation of such a structure, see Fig. S3.[32]

The electronic band structure is presented in Fig. 3, along with the partial density of states for Si and N atoms. It is evident that SiN_4 is a metal in electrical conduction shown in Fig. 3(a). Upshift and downshift Fermi energy level do not alter the metallic nature, suggesting that this compound is an intrinsic metal which does not evolve from a semiconductor. A striking feature is that the energy dispersions along L–Γ–X directions in the Brillouin zone exhibit a parabolic curve, reminiscent of a free electron's behavior. Similar dispersions are often existent in alkali metals and monovalent metals. The effective mass of the delocalized electrons is estimated to be about $1.12m_e$ based on this dispersion, where m_e is the rest mass of an electron. To confirm this, we evaluate the localization extent of the electron by the electron localized function (ELF).[34] The calculated results (Fig. S4[32]) indicate that the electrons lying in the vicinity of Fermi energy are indeed highly delocalized as manifested by the values of ELF, which is well below 0.5, a criterion value for localization. In addition, assuming each N=N bond provides two delocalized electrons, we obtain the total 32 free electrons in one unit cell and electron density is about 2.75×10^{22} cm^{-3}. This is a typical value for a normal metal. To evaluate the electrical conductivity, we calculate the relaxation time of electrons based on Bardeen and Shockley's deformation potential theory,[35,36] which is applicable to the case of delocalized electrons. The calculated details are deposited in the Supplementary Materials.[32] The relaxation time τ is about 7.32×10^{-14} s. The electrical conductivity is then easily obtained to be $\sigma = 5.07 \times 10^5$ S/cm or the resistivity $\rho = 1.97 \times 10^{-6}$ Ω·cm at 300 K. This value is very close to 1.68×10^{-6} Ω·cm for copper and 2.82×10^{-6} Ω·cm for aluminum at 297 K. The thermal conductivity can be estimated to be about 371 W·m^{-1}K^{-1}) using the Wiedemann–Franz law if only the contribution of electrons is taken into account here. Again, it is very close to that for copper at room temperature. If considering the contribution of acoustical branch phonons at low frequencies (Fig. S1), the total thermal conductivity should be higher than the above value.

The partial density of states shown in Fig. 3(b) allows us to analyze the contributions from Si and N

atoms to the metallic characteristic for SiN_4. Apparently, N atoms contribute more states in the vicinity of the Fermi energy than Si atoms. The orbital analysis shown in the bottom panel of Fig. 3(b) indicates that these states are mainly occupied by N delocalized electrons in anti-bonding π^* bands. It is noticed that Si delocalized electrons exist in the σ^* bonds from the Si sp^3 hybridized orbital and N sp hybridized orbital, which lies at the conduction band. This feature indicates that the antibonding σ^* for Si can be occupied probably due to its moderate wide band gap if the density of delocalized electrons is high enough in the compound. Replacing N with C in SiN_4 results in isostructural SiC_4, where SiC_4 tetrahedra are connected by C≡C triple bonds. Band structure calculations indicate that it is a semiconductor with a band gap up to 3.82 eV, see Table 1. This is reasonable since C≡C triple bonds have no delocalized electron left for bonding to Si.

Table 1. Calculated density, band gap, E_c, lattice constant (L), and bond length (BL) for SiN_4, AlN_4, and SiC_4.

	Density (g/cm^3)	Band gap (eV)	E_c (eV/atom)	L (Å)	BL (Å)
SiN_4	0.996	0	−7.156	10.392	1.231_{NN} 1.635_{NSi}
AlN_4	0.799	0	−6.980	11.137	1.223_{NN} 1.804_{NAl}
SiC_4	0.716	3.82	−7.682	11.223	1.226_{CC} 1.817_{CSi}

As SiN_4 can be regarded from cubic close packing of SiN_4 tetrahedra, we also examine its modification formed by hexagonal close packing in terms of the $\cdots$ABAB$\cdots$ sequence. In the hexagonal phase, tetrahedral SiN_4 is also connected by four other via the N=N double bonds. After geometry optimization, we obtain the hexagonal phase of SiN_4 with the lattice constants $a = 7.338$ Å, $c = 12.006$ Å, and space group $P6_3/mmc$, see the crystal structure in Fig. S5.[32] Lattice dynamic and cohesive energy calculation indicate that the hexagonal SiN_4 is stable (Fig. S6[32]). It also has a metal-like feature in the calculated electronic band structure (Fig. S7[32]).

To test the role of the nitrogen dimer in inducing the high electrical and thermal conductivities, we also examine isostructural AlN_4, which has a lattice constant $a = 11.137$ Å after geometry optimization (Fig. S8[32]). Lattice dynamic and cohesive energy calculation results suggest that it should be stable (Fig. S9[32]). Like SiN_4, AlN_4 has N=N double bonds and is metallic in conductivity (Fig. S10[32]). This means that nitrogen dimers can be regarded as a material gene to this class of compounds that exhibit the metal-like behavior, in particular, high electrical and thermal conductivities. Finally, since Si_2CN_4[37,38] and other nitrogen-rich compounds that contain N=N double bonds can be synthesized from organic polymer precursors at proper temperatures and pressure,[39] SiN_4 is likely obtained from the similar route.

In conclusion, to enrich the material genes and fingerprints associated with high electrical and thermal conductivities, we explore a new type of compounds with such properties, and predict that new compounds SiN_4 and AlN_4 with diamond-like structure are stable and metallic. Highly dense delocalized electrons and N=N double bonds are the key factors to realizing the metallic-like conductivity in these compounds because they have a strong tendency to provide a high density of delocalized electrons by forming π^* bonds. These electrons exhibit features in mono-valent metals. Thus nitrogen dimer can be treated as a material gene, that is, a fragment of property-labelled materials. It can be used as a descriptor in determining material properties proposed by Isayev *et al.*,[6] and to construct nitrides with high electrical and thermal conductivities.

References

[1] Nosengo N 2016 *Nature* **533** 22
[2] Mueller T et al 2016 *Rev. Comput. Chem.* **29** 186
[3] Isayev O et al 2015 *Chem. Mater.* **27** 735
[4] Seko A et al 2015 *Phys. Rev. Lett.* **115** 205901
[5] Carrete J et al 2014 *Phys. Rev.* X **4** 011019
[6] Isayev O et al 2017 *Nat. Commun.* **8** 15679
[7] Fujimura K et al 2013 *Adv. Energy Mater.* **3** 980
[8] Mnih V et al 2015 *Nature* **518** 529
[9] Silver D et al 2017 *Nature* **550** 354
[10] Dresselhaus M S and Dresselhaus G 2002 *Adv. Phys.* **51** 1
[11] Novoselov K S et al 2004 *Science* **306** 666
[12] MacDiarmid A G 2001 *Rev. Mod. Phys.* **73** 701
[13] Castro Neto A H et al 2009 *Rev. Mod. Phys.* **81** 109
[14] Le T et al 2017 *Polymers* **9** 150
[15] Abram R A et al 1978 *Adv. Phys.* **27** 799
[16] Graphite is not an intrinsic metal
[17] Vajenine G V et al 2001 *Inorg. Chem.* **40** 4866
[18] Auffermann G et al 2001 *Angew. Chem. Int. Ed.* **40** 547
[19] Auffermann G et al 2006 *Z. Anorg. Allg. Chem.* **632** 565
[20] Toraya H 2000 *J. Appl. Crystallogr.* **33** 95
[21] Du Boulay D et al 2004 *Acta Crystallogr. Sect.* B **60** 388
[22] Sheng X et al 2011 *Phys. Rev. Lett.* **106** 155703
[23] Zhang J et al 2017 *Nat. Commun.* **8** 683
[24] Jo J Y and Kim B G 2012 *Phys. Rev.* B **86** 075151
[25] Hohenberg P and Kohn W 1964 *Phys. Rev.* B **136** B864
[26] Kohn W and Sham L J 1965 *Phys. Rev.* **140** 1133
[27] Perdew J P et al 1996 *Phys. Rev. Lett.* **77** 3865
[28] Langreth D C and Mehl M J 1983 *Phys. Rev.* B **28** 1809
[29] Pfrommer B G et al 1997 *J. Comput. Phys.* **131** 233
[30] Getmanskii I V et al 2017 *J. Phys. Chem.* C **121** 22187
[31] Steglenko D V et al 2017 *Russ. J. Inorg. Chem.* **62** 802
[32] See the Supplemental Material for computational methods and results for cubic SiN_4 (Table S1, Figs. S1, S2, S4), cubic BN_4(Fig. S3), hexagonal SiN_4(Figs. S5–S7), cubic AlN_4(Table S2, Figs. S8–S10) and cubic SiC_4(Table S3, Figs. S11–S14).
[33] Wang H et al 2006 *J. Phys.: Condens. Matter* **18** 10663
[34] Becke A D and Edgecombe K E 1990 *J. Chem. Phys.* **92** 5397
[35] Bardeen J and Shockley W 1950 *Phys. Rev.* **80** 72
[36] Xi J et al 2012 *Nanoscale* **4** 4348
[37] Riedel R et al 1997 *Angew. Chem. Int. Ed.* **36** 603
[38] Sun W et al 2017 *Chem. Mater.* **29** 6936
[39] Schneider S B et al 2012 *Inorg. Chem.* **51** 2366

Supplementary Material: New Type of Nitrides with High Electrical and Thermal Conductivities*

Ning Liu (刘宁)[1,2], Xiaolong Chen(陈小龙)[1,2,3**], Jiangang Guo(郭建刚)[1**],

Jun Deng(邓俊)[1,2], Liwei Guo(郭丽伟)[1]

[1] Research & Development Center for Functional Crystals, Laboratory of Advanced Materials & Electron Microscopy, Beijing National Laboratory for Condensed Matter Physics, Institute of Physics, Chinese Academy of Sciences, Beijing 100190, China

[2] University of Chinese Academy of Sciences, Beijing 100049, China

[3] Collaborative Innovation Center of Quantum Matter, Beijing 100084, China

* This work is financially supported by the National Natural Science Foundation of China (Grant Nos. 51532010, 91422303, 51672306, 51772322) and the National Key Research and Development Program of China (2016YFA0300604), Beijing municipal Science & Technology Commission (Grant No. Z161100002116018), and the Strategic Priority Research Program of the Chinese Academy of Sciences (Grant No. XDB07020100).

** Corresponding author. Email: chenx29@iphy.ac.cn; jgguo@iphy.ac.cn

Text A: Computational Methods and Details

The first-principles calculations were performed with the CAMBRIDGE SERIAL TOTAL ENERGY PACKAGE [1] with the plane-wave pseudopotential method. We adopted the generalized gradient approximation (GGA) in the form of the Perdew-Burke-rnzerhof (PBE) for the exchange-correlation potentials [2]. The ultrasoft pseudopotential with a plane-wave energy cutoff of 500 eV. The first Brillouin zone was sampled with grid spacing of 0.02 $Å^{-1}$.[3] The self-consistent field was set as 5×10^{-7} eV/atom. Both lattice parameters and atomic positions were optimized with the Broyden, Fletcher, Goldfarb, and Shannon (BFGS) method [4] until energy change less than 5×10^{-6} eV/atom, residual force less than 0.01 eV/Å and max stress less than 0.02 GPa. Phonon caculations were performed with the finite-displacement method [5,6] using both GGA-PBE and the local-density approximation (LDA) function [7,8] for comparison. Molecular dynamics simulation based on the velocity Verlet algorithm is performed with time steps of 3 fs for 1.5 ps at 600 K in the NVT ensemble. The cohesive energy, E_c, is

calculated by E_c= [mE(Si)+nE(N)- E(Si_mN_n)]/(m+n), where E(Si), E(N), and E(Si_mN_n) are the energies of Si atom, N atom, and Si_mN_n compound, respectively.

The relaxation-time τ and mobility are calculated based on deformation potential (DP) theory proposed by Bardeen and Shockley [9]. The electrical mobility and relaxation time τ are estimated by the formula, $\mu_\beta = \frac{e\tau_\beta}{m^*} = \frac{2\sqrt{2\pi}eC_\beta\hbar^4}{3(k_BT)^{3/2}E_\beta^2 m^{*5/2}}$, where C_β is the elastic constant, E_β is the DP constant and m^* is the electronic effective mass. By fitting the total energy with respect to volume change, $(E\text{-}E_0)/V_0$ to dilation $\Delta l/l_0$ with $(E\text{-}E_0)/V_0 = C_\beta(\Delta l/l_0)^2/2$, the elastic constant C_β along the transport direction β can be determined. Here V_0 is the cell volume at equilibrium, and l_0 is the lattice constant along direction of β. The DP constant is defined as $E_\beta = \Delta E/(\Delta l/l_0)$, where ΔE is the energy change of the Fermi level with lattice dilation $\Delta l/l_0$ the direction of β. The electrical conductivity is calculated by $\sigma = (ne^2\tau)/ m^*$, where n is the free electron density.

Table S1: Computed cohesive energy for cubic SiN_4-c (*Fd-3m*), hexagonal SiN_4-h (*P6₃/mmc*), Si_3N_4 (*Fd-3m*), Si_3N_4 (*P31c*), Si_3N_4 (*P6₃*), Si_3N_4 (*P6₃/m*) and Si_3N_4 (*I-43d*).

	SiN_4-c (*Fd-3m*)	SiN_4-h (*P6₃/mmc*)	Si_3N_4 (*Fd-3m*)	Si_3N_4 (*P31c*)	Si_3N_4 (*P6₃*)	Si_3N_4 (*P6₃/m*)	Si_3N_4 (*I-43d*)
E_c (eV/atom)	-7.156	-7.164	-8.107	-8.258	-8.258	-8.258	-8.156

Figure S1: The phonon spectrum for cubic SiN4 with GGA (solid blue line) and LDA (dotted red line). Two phonon gaps form due to the large difference of vibration frequency of N-N and Si-N bonds.

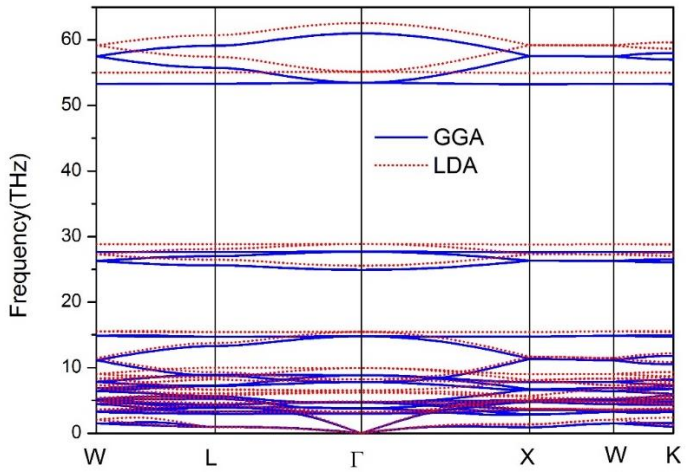

Figure S2: Molecular dynamics simulation based on the velocity Verlet algorithm is performed with time steps of 3 fs for 1.5 ps at 600 K in the NVT ensemble. The inset shows the crystal structure at corresponding time step.

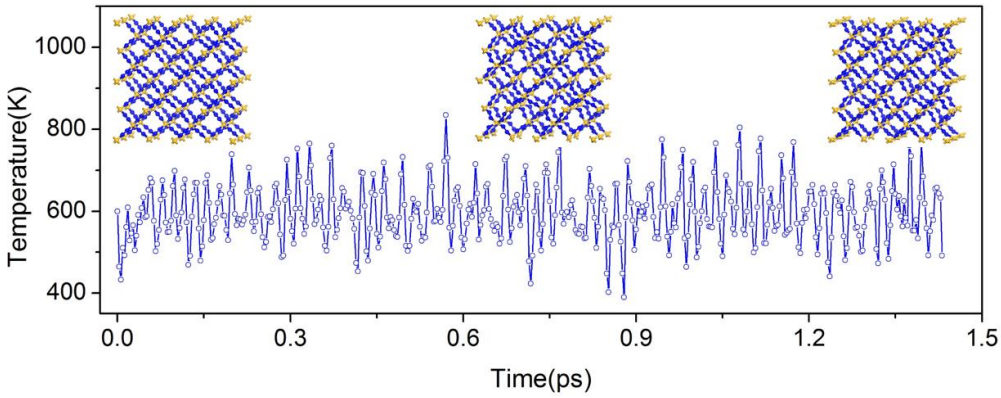

Figure S3: The calculated phonon spectrum for cubic BN_4 compound. The large negative frequency of acoustic branches can be observed.

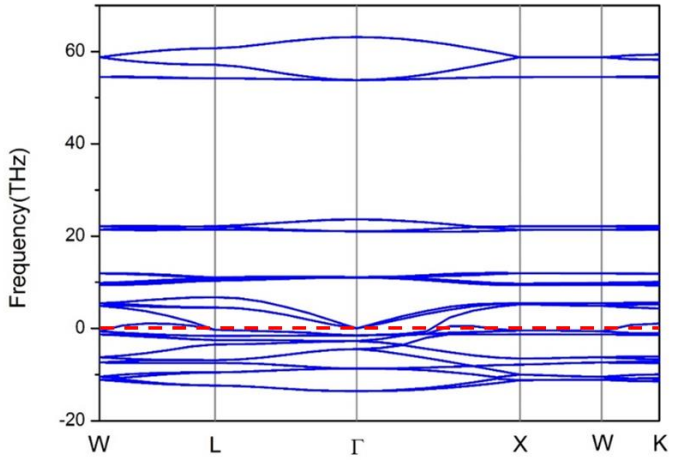

Figure S4: Electron localization function for cubic SiN_4. The values of 0.5 and 1.0 represent fully delocalized (homogeneous electron gas) and fully localized electrons, respectively, while the value of 0.0 refers to very low charge density.[10]

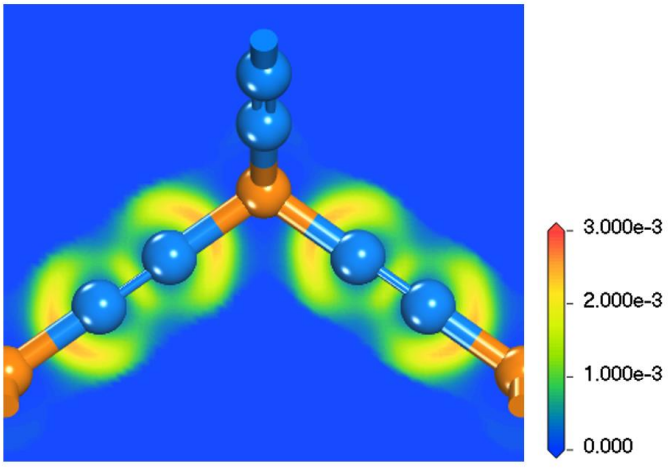

Figure S5: The crystal structure of hexagonal SiN_4, space group *P63/mmc* (No.194) with lattice constant a = 7.431 Å, c = 12.151 Å.

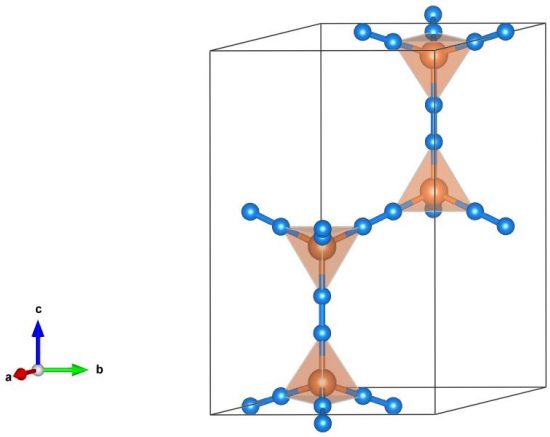

Figure S6: The phonon spectrum for hexagonal SiN_4. The similar phonon gaps are also observed.

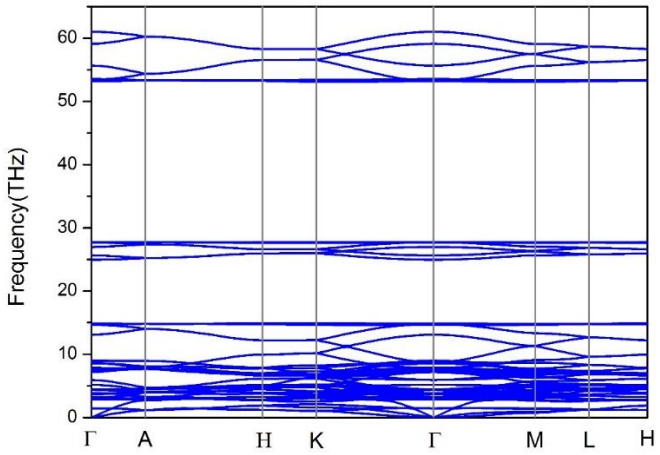

Figure S7: The band structure for hexagonal SiN_4.

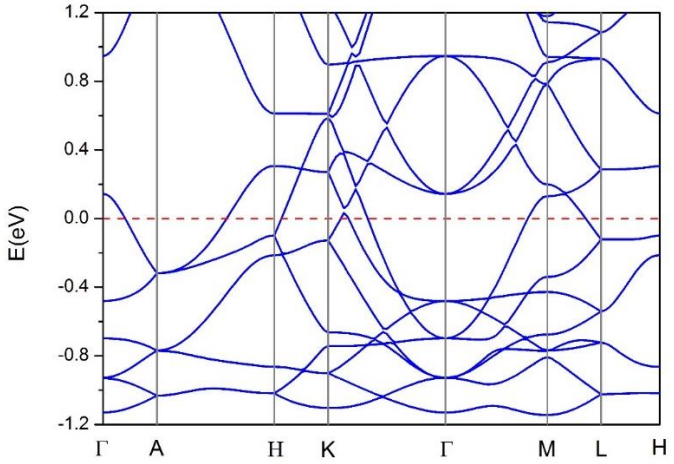

Figure S8: The crystal structure of cubic AlN_4, space group *Fd-3m* (No.227) with lattice constant a = 11.137 Å.

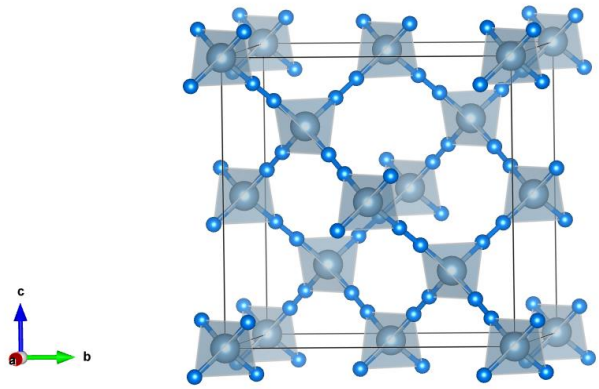

Table S2: Computed cohesive energy (E_c) for AlN_4 (*Fd-3m*), AlN (*P6₃mc*), AlN (*F-43m*), AlN-2D [11], AlN (*Fm-3m*) and AlN (*Cmcm*).

	AlN_4 (*Fd-3m*)	AlN (*P6₃mc*)	AlN (*F-43m*)	AlN-2D	AlN (*Fm-3m*)	AlN (*Cmcm*)
E_c (eV/atom)	-6.980	-7.460	-7.437	-6.957	-7.283	-7.343

Figure S9: The phonon spectrum for cubic AlN_4. No negative frequencies are observed in the acoustic branches.

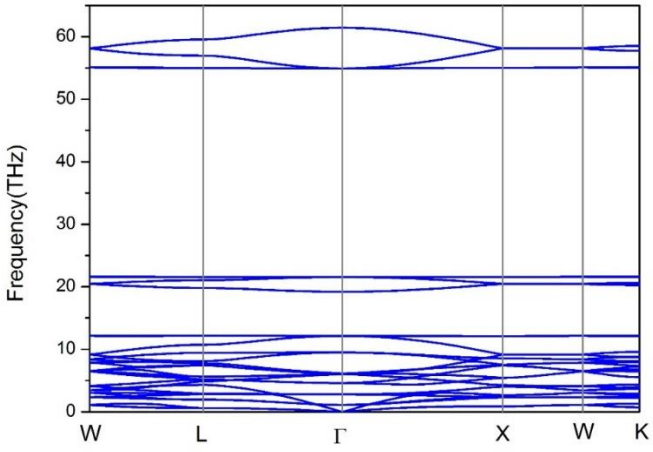

Figure S10: The band structure for cubic AlN_4. The parabolic dispersion also can be observed around Γ point like that of SiN_4.

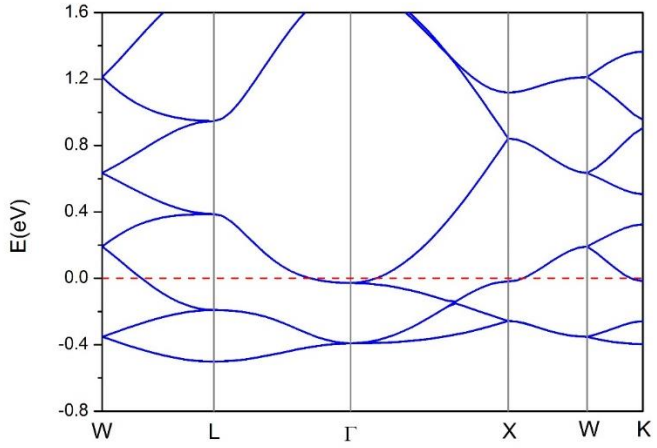

Figure S11: The crystal structure of cubic SiC_4, space group *Fd-3m* (No.227) with lattice constant a = 11.223 Å.

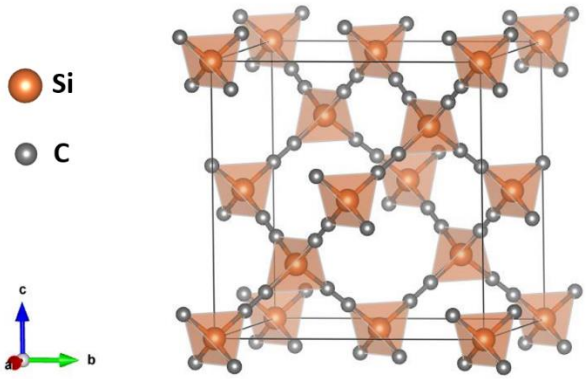

Table S3: Computed cohesive energy (E_c) for SiC_4 (*Fd-3m*), SiC (*6H*), SiC (*2H*), SiC (*3C*) and SiC_2 (*$P4_2/mmc$*).

	SiC_4 (*Fd-3m*)	SiC (*6H*)	SiC (*4H*)	SiC (*2H*)	SiC (*3C*)	SiC_2 (*$P4_2/mmc$*)
E_c (eV/atom)	-7.682	-7.581	-7.581	-7.578	-7.580	-7.570

Figure S12: The phonon spectrum for cubic SiC_4. No negative frequencies are observed in the acoustic branches.

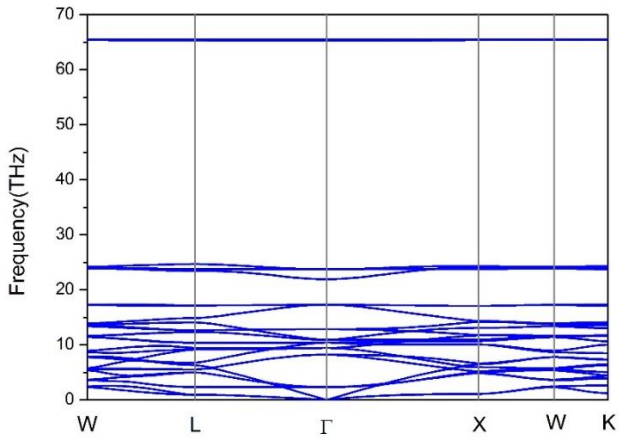

Figure S13: The band structure for cubic SiC_4 with a band gap of 3.82 eV.

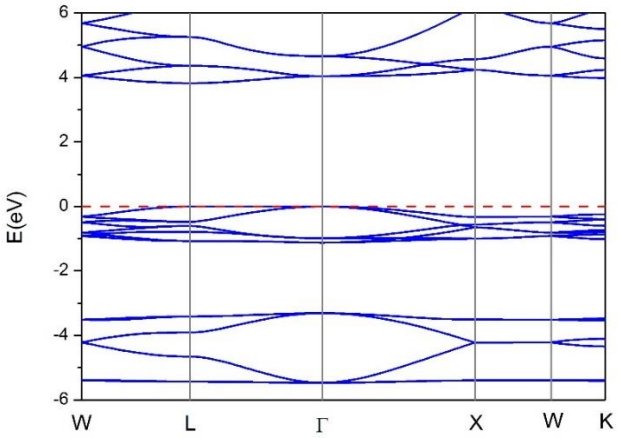

Figure S14: Electron localization function for cubic SiC_4.

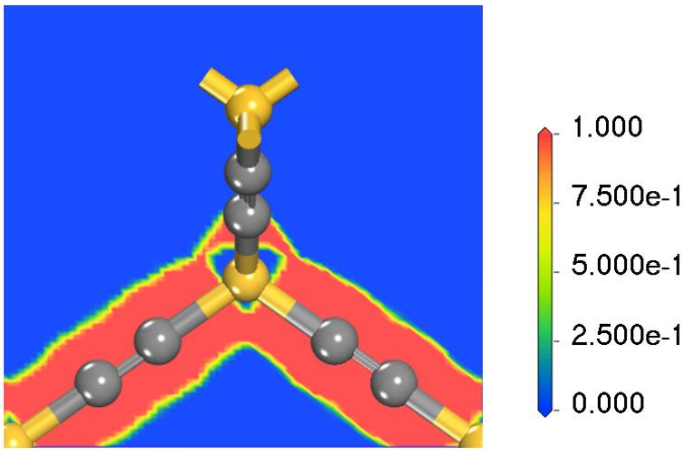

References

[1] Clark S J, Segall M D et al 2005 *Zeitschrift für Kristallographie* **220** 567

[2] Perdew J P, Burke K and Ernzerhof M 1996 *Phys. Rev. Lett.* **77** 3865

[3] Monkhorst H J and Pack J D 1976 *Phys. Rev. B.* **13** 5188

[4] Pfrommer B G, Côté M, Louie S G et al 1997 *J. Comput. Phys.* **131** 233

[5] Frank W, Elsässer C, Fähnle M 1995 *Phys. Rev Lett.* **74** 1791

[6] Parlinski K, Li Z Q, Kawazoe Y 1997 *Phys. Rev. Lett.* **78** 4063

[7] Ceperley D M, Alder B J 1980 *Phys. Rev. Lett.* **45** 566

[8] Perdew J P, Zunger A 1981 *Phys. Rev. B.* **23** 5048

[9] Bardeen J, Shockley W 1950 *Phys. Rev.* **80** 72

[10] Becke A D, Edgecombe K E 1990 *J. Chem. Phys.* **92** 5397

[11] Zhuang H L, Singh A K and Hennig R G 2013 *Phys. Rev. B* **87** 165415